Probabilistic Active Sensing Acousto-Ultrasound SHM Based on Non-Parametric Stochastic Representations

Ahmad Amer
PhD Student
Center for Mobility with Vertical Lift (MOVE)
Rensselaer Polytechnic Institute, Troy, NY, USA

Fotis Kopsaftopoulos
Assistant Professor
Center for Mobility with Vertical Lift (MOVE)
Rensselaer Polytechnic Institute, Troy, NY, USA

ABSTRACT

Existing Structural Health Monitoring (SHM) techniques generally depend on deterministic parameters in order to detect, localize, and quantify damage. This limits the applicability of such systems in real-life situations, where stochastic, time-varying structural response, as well as complex damage types immersed in operational/environmental uncertainties are almost always encountered. Thus, there lies a need for the proposal of statistical quantities and methods for assessing structural health. That is, a holistic probabilistic SHM framework involving damage detection, localization, and quantification, is due if such systems are to become standard on VTOL platforms. In this work, a novel probabilistic approach for active-sensing acousto-ultrasound SHM targeting damage detection and quantification is proposed based on stochastic non-parametric time series representations. Statistical signal processing techniques are used to formulate statistical hypothesis tests, based on which a decision can be made to whether a component is healthy or damaged within pre-defined confidence bounds. The methods presented herein can also be used for damage quantification. The proposed framework is first applied to a notched Aluminum coupon with different damage sizes within an active-sensing, local "hot-spot" monitoring framework. After that, experimental data collected over a stiffened Aluminum panel, representing a sub-scale fuselage component, is analyzed using the probabilistic framework for validation of the proposed methods on more real-life structures. Results show the advantage of the proposed techniques in citing confidence to the decision-making process when compared with state-of-the-art damage indicators. In addition, insights into damage localization within a probabilistic framework are also presented, which may be used as a preliminary step to damage localization algorithms, decreasing the computational cost, and increasing the accuracy of imaging techniques under uncertainty.

INTRODUCTION

Structural Health Monitoring (SHM) for VTOL systems has seen a lot of development in recent years. From the design of "smart" line-replaceable units (Refs. 1, 2) to the integration of embedded sensors within fuselage and blade components (Refs. 3, 4), researchers in the Health and Usage Monitoring Systems (HUMS) community are pushing towards achieving online, full system state awareness. Nonetheless, several challenges persist on the road to achieve this on the structural level. As a global aim, future VTOL aircraft with system-level state awareness should be capable of: detecting, localizing, and quantifying incipient damage at the earliest stages possible. In this context, existing SHM methods face challenges due to (i) stochastic time-variant and non-linear structural response (Refs. 4–6), and (ii) incipient damage types and complex failure modes that can be easily masked by the effects of varying states (Ref. 7), especially in a VTOL environment, where component loading frequencies per flight hour maybe an order of magnitude more compared to fixed-wing platforms (Ref. 8). Thus, there lies a need for the development of a probabilistic SHM framework, where proper analysis, modeling, and understanding of stochastic signals under varying states and damage characteristics (type/size/orientation) is achieved for enabling full transformation to condition-based maintenance schemes and life-cycle state awareness.

To this end, the problem of incorporating statistical inference within an active sensing, guided-waves SHM framework has been addressed through two contexts: statistical distribution of damage-related features (also known as *probabilistic SHM*), and reliability quantification of SHM systems.

The postulation of statistical significance of SHM measurements can be realized via the development of probabilistic SHM methods. Studies utilizing probabilistic active-sensing techniques in SHM are quite limited compared to those using deterministic approaches, although probabilistic vibration-based SHM methods have attracted the interest of the research community. A recently-proposed active sensing method for achieving online probabilistic SHM involves the application of Bayes' theorem (Ref. 9). In this approach, a specific model (mostly parametric) is updated based on the likelihood func-

Presented at the Vertical Flight Society 75th Annual Forum & Technology Display, Philadelphia, Pennsylvania, May 13–16, 2019.

tion applied to existing data, which compares the probability distribution of the *previous* signal features space to *current* signals. The distribution of those damage-related features can either be assumed, or formulated using distribution estimation techniques. Todd and coworkers (Ref. 10) used this approach for localizing simulated damages (9 holes) on a stiffened aluminum panel with 7 piezoelectric sensors within a pitch-catch framework. Assuming the raw data represents stochastic Gaussian processes, systematic data processing was done to transform each raw waveform into a feature, which is governed by Rayleigh statistics. After that, a uniform prior probability on the location of the holes was assumed, and then updated using the updated features space and distribution parameters. Another similar approach by the same group of researchers (Ref. 11) included kernel density estimation to achieve the probability density function of the locations of damage (instead of assuming normal distribution), and the use of the well-known statistical techniques of noise-immersed signal detection (Ref. 12) in order to apply the theoretical Receiver Operating Characteristics (ROC) curves of binary hypothesis testing to a Localizer statistic, formulating an LOC. Equipped with either of these methods for estimating the distribution of damage locations using the features space, Bayesian updating was applied as indicated above. Note that, using the theoretical ROC approach, other statistics can be used for damage detection, such as the Power Spectral Density (PSD) using the Fast Fourier Transform (FFT) or the Short Time Fourier Transform (STFT) algorithms (Ref. 13). On the damage quantification side, Yang *et al.* (Refs. 14, 15) used Bayesian updating for crack size quantification in 6 Al plates having notches with increasing lengths within an active sensing approach. Normalized amplitude and phase changes in the first-arrival wave mode (S0) in the signals were used as the parameters in a linear model that predicted damage size. Having initially calculated the parameter values from the experiments, Monte Carlo simulations were then used to fit the parameters to a probability distribution to be able to proceed with Bayesian updating of the notch size model. Similar strategies have been demonstrated for estimating delamination propagation in composites (Ref. 16). The major advantage of all of the reviewed approaches lies in the direct extraction of confidence intervals for the detection, localization, and quantification capabilities of SHM. Furthermore, these approaches show promise in quantifying reliability without the need for NDE testing.

As for reliability quantification, most approaches proposed to date are examined through an analogy to the well-developed Probability of Detection (POD) methodology for Non-destructive Evaluation (NDE) reliability assessment (Ref. 17). Because the NDE POD estimation process, as outlined in MIL-HDBK-1823A (Ref. 18), cannot be directly applied to SHM systems due to the issue of dependant measurements of a single SHM system, as well as the impractical nature and cost of installing many independent SHM systems (Refs. 17, 19, 20), many of the conducted studies attempt to adapt available SHM data to the NDE POD standards. On the experimental side, some researchers proposed the use of parametric models for each SHM unit in order to incorporate dependence into the POD calculation method (Ref. 21), whilst others directly extracted data from many coupons outfitted with identical SHM systems (Ref. 17) in order to quantify the reliability of such an approach in POD estimation. On the computational side, researchers proposed the use of a Model-Assisted POD (MAPOD) (Refs. 19,22) in order to generate independent SHM data for direct application of POD standards. Using models, identical properties of the different SHM systems would prevent the incorporation of system-induced measurement error, while assuring independence. Indeed, the majority of studies applying POD to SHM use some sort of a Health Indicator (HI) in order to interrogate a specific structure, i.e. a deterministic metric that allows only for a damage/no damage decision scheme with no regard to estimation uncertainty or operational/environmental conditions. Thus, the formulation of POD in this case only allows for reliability quantification. There lies a lack of formulating a statistical inference framework that is inherent to the SHM metrics being used for damage detection, quantification, and localization, i.e. there are no treatments to the intrinsic statistical properties associated with active-sensing damage-sensitive features within SHM measurements.

As indicated in the discussion above, in order to achieve probabilistic SHM, a statistical quantity needs to be defined for the system so that probabilistic information can be extracted. This implies the existence of some stochastic model of the system, which describes system dynamics within a statistical framework. In this context, statistical time series methods have been proposed and attracted the interest of the vibration-based SHM community in order to model the stochastic vibrational response of a structure and enable damage detection, localization and quantification with predetermined confidence intervals (Refs. 23–25). In such methods, both parametric and non-parametric models can be used (Refs. 23, 26). Using finitely-parametrized representations of the system, parametric time series models may result in improved accuracy compared to their non-parametric counterparts, and their parameters may be correlated to physical system parameters, such as modal parameters (Ref. 27). However, the identification of parametric models is generally more complex and requires significant user experience (Ref. 23). On the other hand, non-parametric time series models are straightforward in terms of implementation, require little-to-no user expertise in model building and assessment, and are computationally efficient. However, the added simplicity comes at the potential cost of accuracy and robustness to varying operating/environmental conditions and uncertainty.

In this work, a novel probabilistic approach for active-sensing acousto-ultrasound SHM targeting damage detection and quantification is proposed based on the non-parametric modeling of the wave signals, which allows for the quantification of estimation uncertainties even from a single data set. Experimental data is collected within an active-sensing, local "hot-spot" monitoring framework over a notched-Aluminum plate (benchmark test), as well as a stiffened Aluminum panel (simulating a sub-scale fuselage component) under different

damage scenarios. Non-parametric spectral models incorporating theoretical and experimental estimation uncertainties are used for damage detection and quantification. Results are compared with those of state-of-the-art damage indicators and the differences are discussed within the context of probabilistic SHM. In addition, insights into statistical damage localization, based on the same approach, are also presented, which may be used as a preliminary step to probabilistic damage localization algorithms, decreasing the computational cost while increasing the accuracy of imaging techniques under uncertainty. To the authors' best of knowledge, the use of non-parametric models for active-sensing guided-wave probabilistic SHM has not been previously proposed. The major contributions of this study with respect to previous efforts in the literature can be summarized as follows:

- The formulation of a probabilistic damage detection and quantification framework based on non-parametric models of guided-wave active-sensing SHM data, which have the advantage of simplicity and computational efficiency.
- The extraction of statistical confidence intervals directly from the data, even when only a single finite data set is available, without the need for time-consuming and costly ground-based NDE testing nor the requirement for the availability of many data sets.
- The application of the proposed models to damage detection and quantification, with insights into its benefits for damage localization, all within a probabilistic framework.

NON-PARAMETRIC TIME SERIES MODELS

Non-parametric modeling of dynamic systems is based on the use of the time-domain Auto-/Cross-Covariance Functions (A/CCF), or their frequency-domain counterparts, the Auto-/Cross-Spectral Densities (Ref. 28). In the later case, several metrics can be used to estimate the Power Spectral Density (PSD) of a signal, including the periodogram, the Blackman-Tukey, the Welch, and the Thompson estimators (Refs. 29,30). Because the signals used in the estimation are finite in nature, each of these metrics results in an estimated PSD, in contrast to the true PSD of the system. As such, each one has its own estimation confidence intervals, which are used to define the estimation uncertainty in calculating the PSD. In this context, one of the widely-used PSD estimators is the modified periodogram estimator using Welch overlapping windows (Ref. 31), also known as the Welch PSD estimator (Ref. 30). The Welch PSD estimator, with respect to frequency ω, of a time series signal ($x[t]$) is based on the averaging of multiple windowed periodograms using properly selected windows ($w[\tau]$) with 50% overlap, and is calculated as follows (Refs. 31,32):

$$\widehat{S}_{xx}(\omega) = \frac{1}{KLUT}\sum_{i=0}^{K-1}|T\sum_{n=0}^{L-1}w[n]\widehat{x}[n+iD]exp(-j2\pi\omega nT)|^2 \quad (1)$$

with

$$U = \frac{1}{L}\sum_{n=0}^{L-1}w^2[n], \quad \widehat{x}[t] = x[t]-\widehat{\mu}_x, \quad N = L+D(K-1) \quad (2)$$

and N, K, L, D, and T being the total number of signal time points, the number of utilized windows, the size of each window, the number of overlapping data points in each window, and the time period of the signal, respectively, and $\widehat{\mu}_x$ the mean of the signal (the hat indicates an estimated variable). The mean and variance of the Welch PSD estimator are described as follows:

$$E[\widehat{S}_{xx}(\omega)] = \frac{1}{2\pi LU}S_{xx}(\omega)|W(\omega)|^2 \quad (3)$$

$$Var[\widehat{S}_{xx}(\omega)] = \frac{9}{16}\frac{L}{N}S_{xx}^2(\omega) \quad (4)$$

where $W(\omega)$ is the Fourier transform of the window function. It can be shown that the Welch PSD estimator is asymptotically unbiased and consistent (Ref. 30). A different, but similar, algorithm to compute the PSD involves the use of a sliding window with overlap exceeding 50%, which gives PSD results that are both frequency- and time-dependant. This algorithm is the Short-Time Fourier Transform (STFT), and, written in a form similar to the Welch estimation, it can be applied as follows:

$$\widehat{S}_{xx}(\omega,\tau) = \frac{1}{KLUT}\sum_{i=0}^{K-1}|T\sum_{n=0}^{L-1}w[n-\tau]\widehat{x}[n+iD]exp(-j2\pi\omega nT)|^2 \quad (5)$$

STATISTICAL DAMAGE DETECTION AND QUANTIFICATION

Analysis of guided-wave sensor signals using non-parametric time series methods, such as the Welch PSD estimator, whilst incorporating statistical tools, has been reported previously for vibration-based SHM systems by Kopsaftopoulos and coworkers (Refs. 33–35). Figure 1 presents the main ideas behind a probabilistic SHM framework that employs Statistical Hypothesis Test (SHT) for inference using time series models. As shown, during a baseline phase, using a time series model (parametric or non-parametric), one can estimate a characteristic quantity $\widehat{Q}$ for the healthy ($\widehat{Q}_0$), as well as different predefined damage cases ($\widehat{Q}_A$, $\widehat{Q}_B$,...). After that, during the inspection phase, the same characteristic quantity would be extracted from the current/unknown signals ($\widehat{Q}_u$), and a statistical hypothesis test is applied to check –in a statistical sense– for deviation of $\widehat{Q}_u$ from $\widehat{Q}_0$ (damage detection) and its statistical similarity to one of the predefined damage quantities: $\widehat{Q}_A$, $\widehat{Q}_B$,... (damage classification). Note here that the different damage cases can be different sizes or types of damage; they can also be different locations and magnitudes of damage thus extending the application of this method to damage localization and quantification.

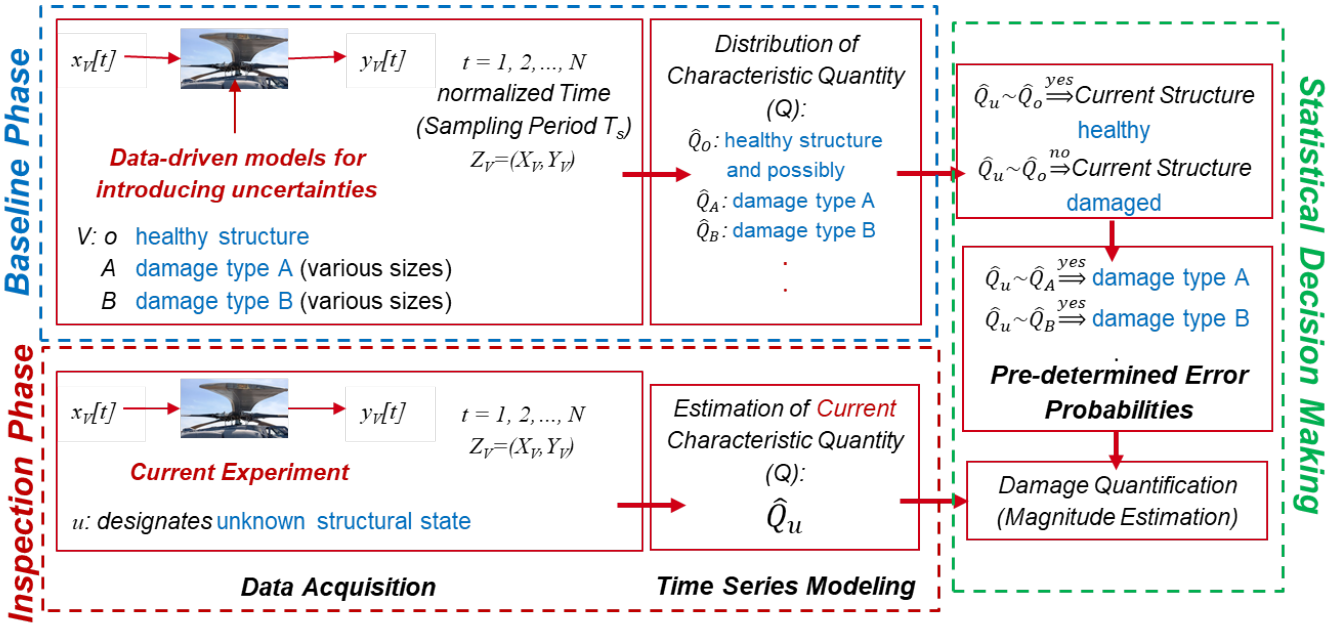

Fig. 1. Workframe for statistical time series methods for structural health monitoring (Ref. 33).

PSD-based Method

Based on the non-parametric PSD-based method and the corresponding SHT schemes (Ref. 33), damage detection is tackled via identifying changes in the PSD of the measured wave propagation signals or properly determined wave packets. The methods characteristic quantity thus is $Q = S_{yy}(\omega) = S(\omega)$, with ω designating frequency. The main idea is based on the comparison of the current structures response PSD, $S_u(\omega)$, to that of the healthy structures, $S_u(\omega)$. In the case of active sensing SHM, appropriate wave packets corresponding to the modes of wave propagation can be used as the signals for the estimation of the PSD. In this method, the statistical PSD model's characteristics are based on the theoretical analysis of the Welch based PSD estimator (Ref. 29). Damage detection then is based on the following statistical hypothesis testing problem (Ref. 33):

$$\begin{aligned} H_o &: S_u(\omega) = S_o(\omega) \quad \text{(null hypothesis: healthy)} \\ H_1 &: S_u(\omega) \neq S_o(\omega) \quad \text{(alternative hypothesis: damaged)} \end{aligned} \tag{6}$$

However, because the true values of the PSD are not known, corresponding estimated quantities are used instead ($\widehat{Q}$). It can be shown that the Welch PSD estimator will have the following property (Ref. 29):

$$2K\widehat{S}(\omega)/S(\omega) \sim \chi^2(2K) \tag{7}$$

Thus, it can be shown that the following relation will follow the $\mathscr{F}$ distribution with $(2K, 2K)$ degrees of freedom:

$$F = \frac{\widehat{S}_o(\omega)/S_o(\omega)}{\widehat{S}_u(\omega)/S_u(\omega)} \sim \mathscr{F}(2K, 2K) \tag{8}$$

such that $S_u(\omega)$ and $S_o(\omega)$ are the true PSDs of the current and healthy signals, respectively, and they are both statistically equal under the null hypothesis. Then, selecting the appropriate confidence intervals (1-α), where α is Type I error (*false alarm*), one may utilize the following decision-making process:

$$\begin{aligned} &\text{if} f_{\frac{\alpha}{2}}(2K,2K) \leq F = \frac{\widehat{S}_o(\omega)}{\widehat{S}_u(\omega)} \leq f_{1-\frac{\alpha}{2}}(2K,2K) \quad (\forall\, \omega): \\ &\quad H_o \quad \text{is accepted (healthy structure)} \\ &\qquad\qquad \text{Else} \\ &\quad H_1 \quad \text{is accepted (damaged structure)} \end{aligned} \tag{9}$$

with $f_{\frac{\alpha}{2}}$, $f_{1-\frac{\alpha}{2}}$ designating the $\mathscr{F}$ distributions $\frac{\alpha}{2}$ and $1-\frac{\alpha}{2}$, respectively, critical points (f_α is defined such that Prob$(F \leq f_\alpha) = \alpha$).

Modified PSD-based Method

In certain cases, more than a single data set is available for a given state of the component being monitored under namely constant operating/environmental conditions (which is the case for closely spaced sampling events). This would then allow for the incorporation of experimental statistics into the estimation of the PSD, such as the sample mean:

$$E[\widehat{S}_o(\omega)] = \frac{1}{M}\sum_{h=1}^{M} \widehat{S}_o(\omega) \tag{10}$$

with M designating the number of healthy data sets used in the Welch-based estimation of the PSD. And since the expectation of a number of healthy data sets would just surmount to the true PSD for a large M, then the following property of the sample mean estimator can be inferred:

$$2KME[\widehat{S}_o(\omega)]/S_(\omega) \sim \chi^2(2KM) \tag{11}$$

In such a case, one can define a mean-enhanced F statistic by replacing the Welch PSD estimate with the mean of the estimates of M number of data sets taken for the healthy state:

$$F_m = \frac{E[\widehat{S}_o(\omega)]/S_o(\omega)}{\widehat{S}_u(\omega)/S_u(f)} \sim \mathscr{F}(2KM, 2K) \qquad (12)$$

Similarly, under the null hypothesis, $S_o(\omega)$ and $S_u(\omega)$ would be statistically equal, and selecting the appropriate confidence level, the decision making scheme can be setup as follows:

$$\begin{aligned} &if\, f_{\frac{\alpha}{2}}(2KM,2K) \leq F_m = \tfrac{E[\widehat{S}_o(\omega)]}{\widehat{S}_u(\omega)} \leq f_{1-\frac{\alpha}{2}}(2KM,2K) \quad (\forall\, f): \\ &\quad H_o \quad \text{is accepted (healthy structure)} \\ &\qquad\qquad \text{Else} \\ &\quad H_1 \quad \text{is accepted (damaged structure)} \end{aligned} \qquad (13)$$

with $f_{\frac{\alpha}{2}}$, $f_{1-\frac{\alpha}{2}}$ designating the $\mathscr{F}$ distributions $\frac{\alpha}{2}$ and $1-\frac{\alpha}{2}$, respectively, critical points (f_α is defined such that Prob$(F \leq f_\alpha) = \alpha$).

EXPERIMENTAL SETUP

The Components

In this study, the models and corresponding damage detection methods presented above were applied to two components with different damage cases. The first one (notched Al plate) was utilized as a benchmark test to validate the proposed models. The second component (sub-scale Al fuselage part) was used as a more realistic case to test the applicability of the models on more complex structures.

Al Plate 6061 Aluminum 152.4 × 254 mm (6 × 10 in) coupons (2.36 mm/0.093 in thick) (McMaster Carr) with a middle hole having a diameter of 0.5 in were used for the notched-Al benchmark experiments to test the analysis technique. 6 single-lead zirconate titanate (PZT) SMART Layers (type PZT-5A) designed and fabricated by Acellent Technologies, Inc the Al plate as shown in Figure 2a using Hysol EA 9394 adhesive. The employed PZT actuators/sensors are 3.175 mm (1/8 in) in diameter and 0.2 mm in thickness. A 2 mm notch was cut extending from the hole of the Al plate with an end mill. Then, the notch was elongated with 2-mm increments up to 20 mm using a 0.81 mm (0.032 in) handsaw.

Sub-scale Al Fuselage Component A 609.6 × 609.6 mm (24 × 24 in) Al panel (0.81 mm/0.032 in thick), fitted with three 25.4 × 25.4 mm (1 × 1 in) stringers was used as a sub-scale fuselage component. Two 8-sensor SMART layers (Acellent Technologies, Inc) were installed using Hysol EA 9394 adhesive on either side of one of the stringers on the fuselage component as shown in Figure 2b. To simulate damage, 5 damage levels (DLs) were used. Firstly, the bottom side of rivet A holding down the stringer between the sensor layers was partially cut out using a hand saw (DL I), then the bottom was completely filed (DL II). After that, rivet A was partially popped out using a hammer (DL III), then completely removed (DL IV). Finally, rivet B was also partially popped out (DL V).

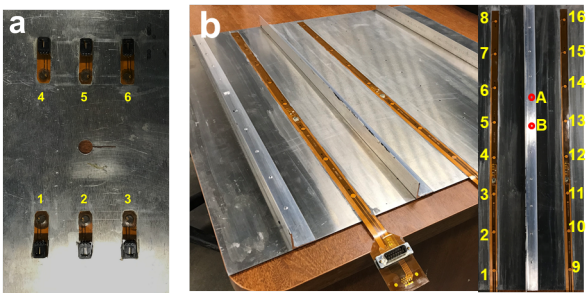

Fig. 2. The two experimental coupons used in this study: (a) notched Al plate and (b) sub-scale fuselage component.

The Test Setup

Actuation signals in the form of 5-peak tone bursts having an amplitude of 90 V peak to peak and various center frequencies were generated in a pitch-catch configuration and 20 data sets per structural case were collected at a sampling rate of 24 MHz using a ScanGenie III data acquisition system (Acellent Technologies, Inc). Data sets were then exported to MATLAB for analysis.[1]

RESULTS AND DISCUSSION

Benchmark Test: Notched Al Plate

The proposed non-parametric methods were first applied to the notched Al plate data sets for damage detection and quantification using guided-wave active sensing SHM. Examining one of the actuator-sensor paths being directly affected by the notch (see Figure 2a for sensor numbering), Figure 3 panels a and b show samples of the full signal and the S0 mode only, respectively, for the signal received at sensor 5 when sensor 3 was actuated with 250 kHz center frequency (path 3-5) for different notch sizes. Generally, it can be observed that a decrease in amplitude, as well as a very slight shift in frequency is observed as the notch increases in length. Figure 4 shows the evolution of the corresponding damage indices (DIs) as calculated using the Root Mean Square Deviation (RMSD) and two state-of-the-art DI's from the literature, as proposed in (Ref. 36) and (Ref. 17). All 20 datasets for each notch size were used for the DI calculations. It can be seen that the DIs follow the increase in notch size (damage quantification), giving a single value for every damage case. The purpose of this approach is to detect the existence of a crack and quantify its size. However, the reliability quantification, i.e. the extent to which a specific deterministic DI-based approach accurately determines the characteristic size of damage can only be quantified by examining the DI-based results for every damage case against those of NDE techniques that can determine damage size within a POD-based framework. As shown, even for a controlled lab environment, the values of the DIs for the same case change with different measurements,

[1] Matlab version R2018a, functions *pwelch.m* (window size: 80-130; nfft: 5000; noverlap: 50%) and *spectrogram.m* (window size: 400-900; nfft: 960; noverlap: 95%).

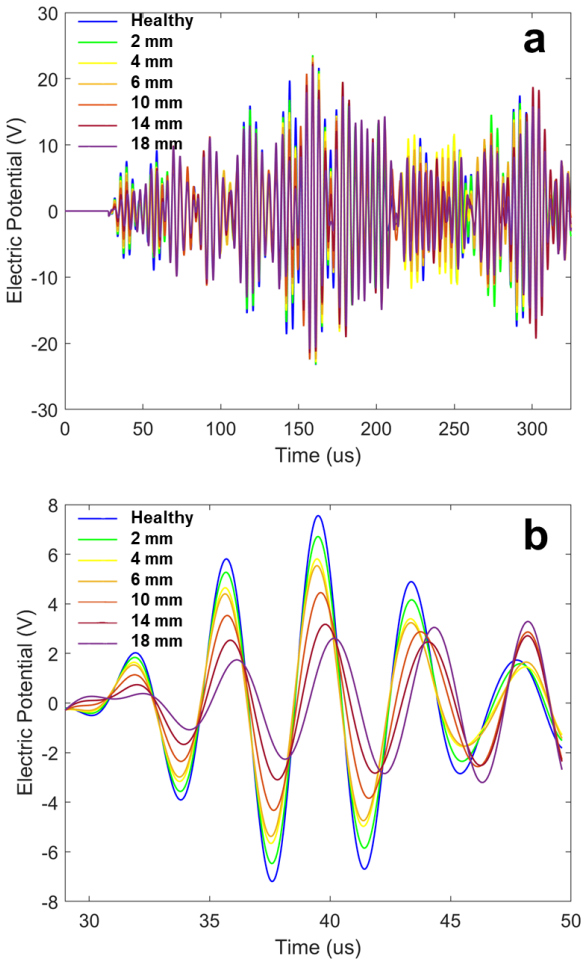

Fig. 3. Notched Al plate: Indicative signals from the 3-5 path at 250 kHz (actuation center frequency) and for different notch sizes showing (a) the full signal, and (b) the S0 mode.

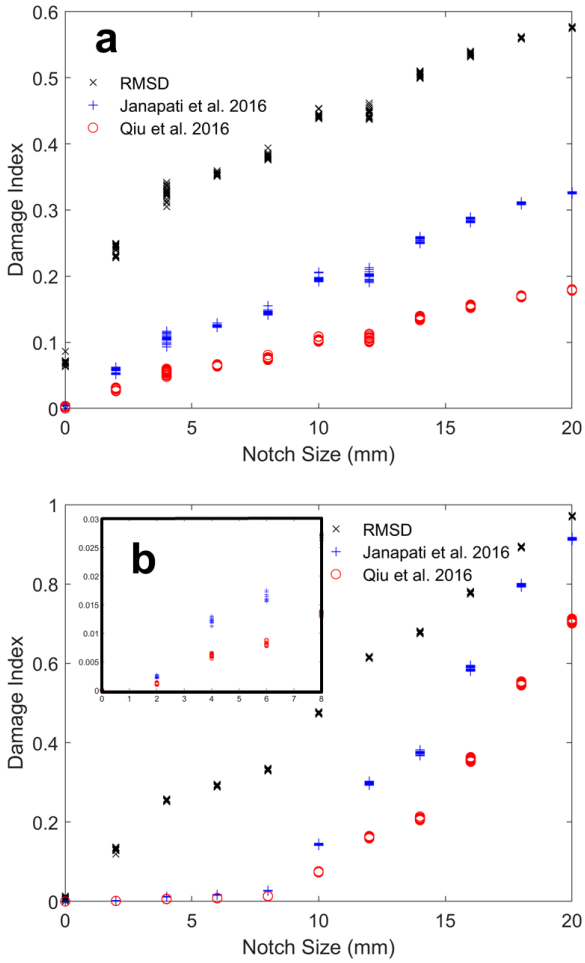

Fig. 4. Notched Al plate: Indicative results for three Damage Indices for the 3-5 signal path and different notch sizes for (a) the full signal and (b) the S0 mode only.

making the decision of damage/no damage quite challenging. Furthermore, no uncertainty estimation and quantification is addressed to allow for the finite nature of the sampled data or the environmental/operating conditions.

Figure 5a and 5b show the Welch PSD estimation for the same 3-5 data set along with 95% statistical confidence intervals (Ref. 29). As shown, both plots show, as expected, the characteristic peak at the frequency of actuation (250 kHz). In addition, a theoretical estimation uncertainty can be clearly defined, such that any signal falling between the confidence intervals will be deemed healthy with 95% confidence, i.e. with an 0.05 α level (type I error or false alarm probability). This estimation of the confidence intervals is made possible due to the stochastic nature of the Welch-based PSD estimate used in this study. As such, some notch sizes might go undetected, as is the case with the 2 mm and the 4 mm notch damages.

Following the formulation of the F and F_m statistics presented in the previous section, damage detection was addressed via the postulated statistical hypothesis testing procedures. Figures 6a and 6b present the results of the F and F_m statistics, respectively, for the 3-5 path for different notch sizes (note that only the first arrival wave packet, i.e. the S0 mode, was used in these figures). In these Figures a damage is detected when the test statistic exceeds the dashed horizontal lines. The first thing to observe is that the proposed statistics are capable of detecting notch damages beyond 6 mm in length with 95% confidence. The second observation is that not all frequencies are sensitive to damage. In addition, the most damage-affected frequencies do not coincide with the actuation frequency used in this analysis (250 kHz), which hints on the complex dynamics involved. Nonetheless, this approach shows promise in differentiating between healthy and damaged cases within a probabilistic framework and predetermined confidence levels.

Looking further into both panels of Figure 6, it can be observed that the F_m statistic has narrower confidence intervals for the same type I error probability $\alpha = 0.05$, as evident from the detection of the 6-mm notch damage. This is expected given the more accurate the sample mean of Welch-based PSD estimates is for an estimate of the system's spectral

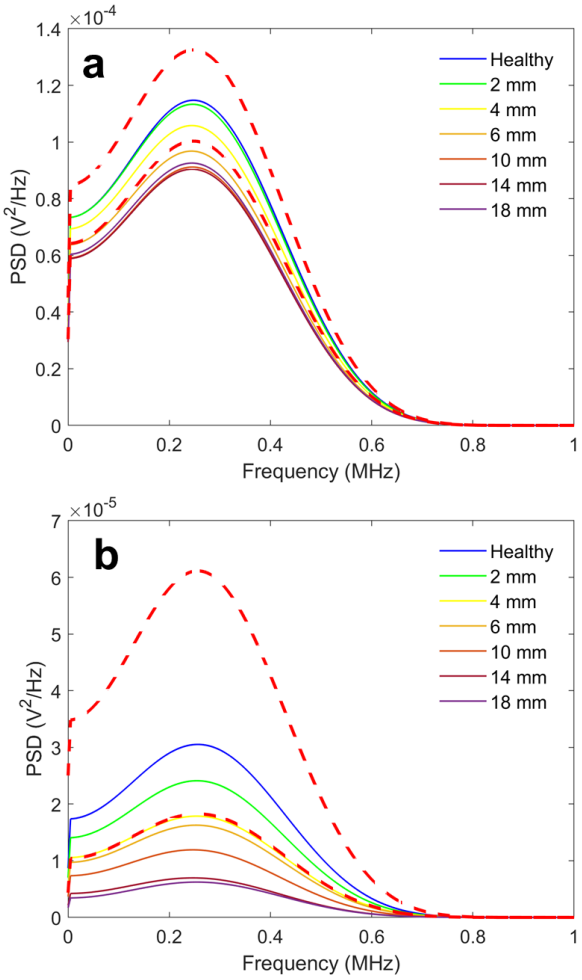

Fig. 5. Notched Al plate: Indicative Welch-based PSD estimates for the 3-5 signal path (250 kHz center frequency) for different notch sizes for (a) the full signal, and (b) the S0 mode.

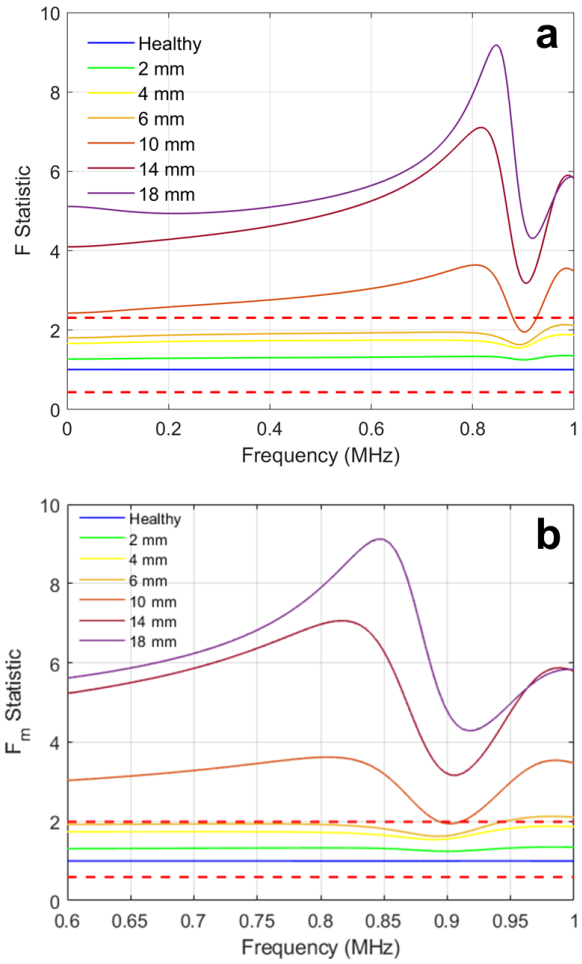

Fig. 6. Notched Al plate: Indicative damage detection results for S0 mode of path 3-5 under 250 kHz actuation via the (a) F and (b) F_m statistics. The dashed horizontal lines indicate the damage thresholds at the 95% confidence level.

density, compared to the Welch-based PSD estimate based on a the theoretical analysis, i.e. $E[\widehat{S}_o(\omega)]$ compared to $\widehat{S}_o(\omega)$). The use of the sample mean of the PSD estimates under several realizations can potentially account for varying operating/environmental conditions, when a signals representative of the admissible conditions are available.

This advantage that the F_m statistic has over the F statistic can also be seen when analyzing actuator-sensor paths that do not intersect damage, i.e. the signals would not be extensively affected by damage. Figure 7 panels a and b show the S0 mode signals and the corresponding DIs, respectively, for path 5-1. As can be observed, the values of the DIs are a fraction of what was observed from Figure 4b. Furthermore, the DI profiles for all three DI formulations do not follow the increase in notch size. This behavior has been observed in previous studies (Ref. 17) and is due to the fact that after a specific damage size, further increasing it does not affect the wave propagation of specific paths that may or may not interest damage.

Figure 8 panels a-c present the Welch-based PSD, F and F_m statistics of the same path, respectively. As shown, using the F statistic, a decision of accepting the null hypothesis (healthy structure) for all cases was reached (because the statistic falls within the "healthy" confidence intervals for all cases and frequencies). Therefore, the F statistic is not able to detect these damages at the 95% confidence level. From the F_m plot, both the 10 and 14 mm cases were correctly determined as damaged. The fact that the 18-mm notch goes undetected, whilst smaller notches are detected (also apparent in Figure 7b from the decline of the values of all DIs for notch sizes more than 10 mm), is related to the fact that this path does not cross the damage, making the effect of damage on this wave propagation path more complex to be clearly detected and quantified. Nonetheless, these observations show the benefit that the F_m statistic might have under the conditions mentioned above. Finally, carrying out both hypothesis tests for all available data sets for each case, false alarm and missed fault percentages were extracted. None of the healthy case data sets were deemed damaged (false alarm rate equal to zero), which is expected given the controlled lab environment in which the tests were carried out. Table 1 shows the summarized missed

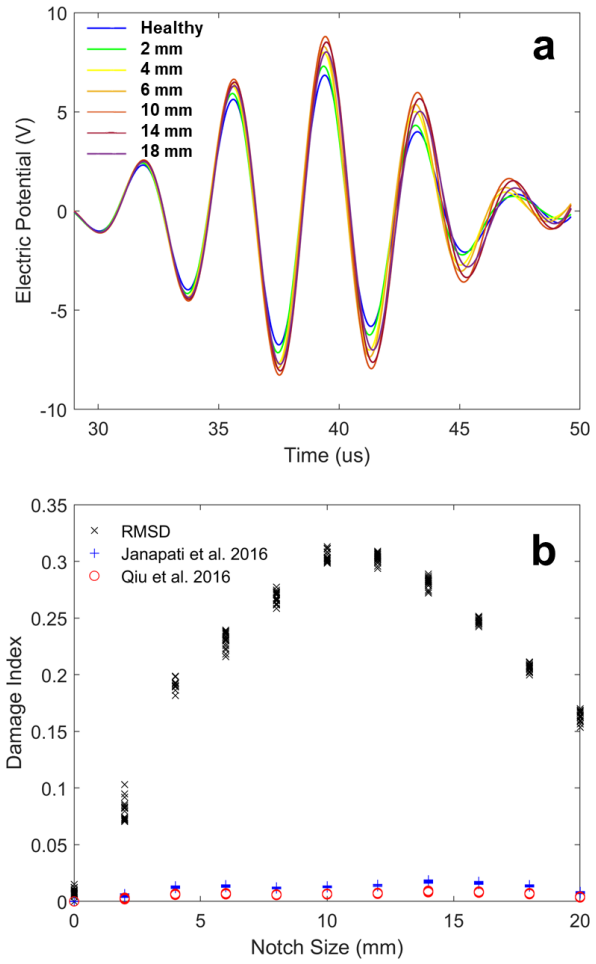

Fig. 7. Notched Al plate: (a) The S0 signal and (b) the corresponding DIs for path 5-1 under 250 kHZ actuation.

faults percentages for select actuator-sensor paths.

As mentioned, the STFT algorithm has the advantage over the Welch PSD estimation in retaining time points in the evaluation of the PSD; that is, the evolution of the PSD across the chosen windows can be captured using the STFT PSD. Figure 9a presents the STFT estimation for the first wave packet (S0) in the path 3-5 (damage intersecting) under different notch sizes, while Figure 9b depicts the corresponding results for path 5-1 (non-intersecting damage). It can be observed that, for the damage intersecting path (3-5), there is a decrease in the PSD magnitude as notch size increases for all frequencies, which is similar to the observed trend from the Welch PSD estimations (see Figure 5b). This is due to scattering effects that occur at/around the damage, where less energy would reach the sensor in the presence of the notch. It can be also readily concluded from the separation between the healthy and damaged boxes that this wave propagation path exhibits a clear distinction between the healthy and the damaged states.

Examining paths that do not intersect damage (Figure 9b), the opposite trend in the development of the STFT PSD magnitude versus notch size can be observed up till a notch length of 10 mm, after which the PSD median value starts to drop.

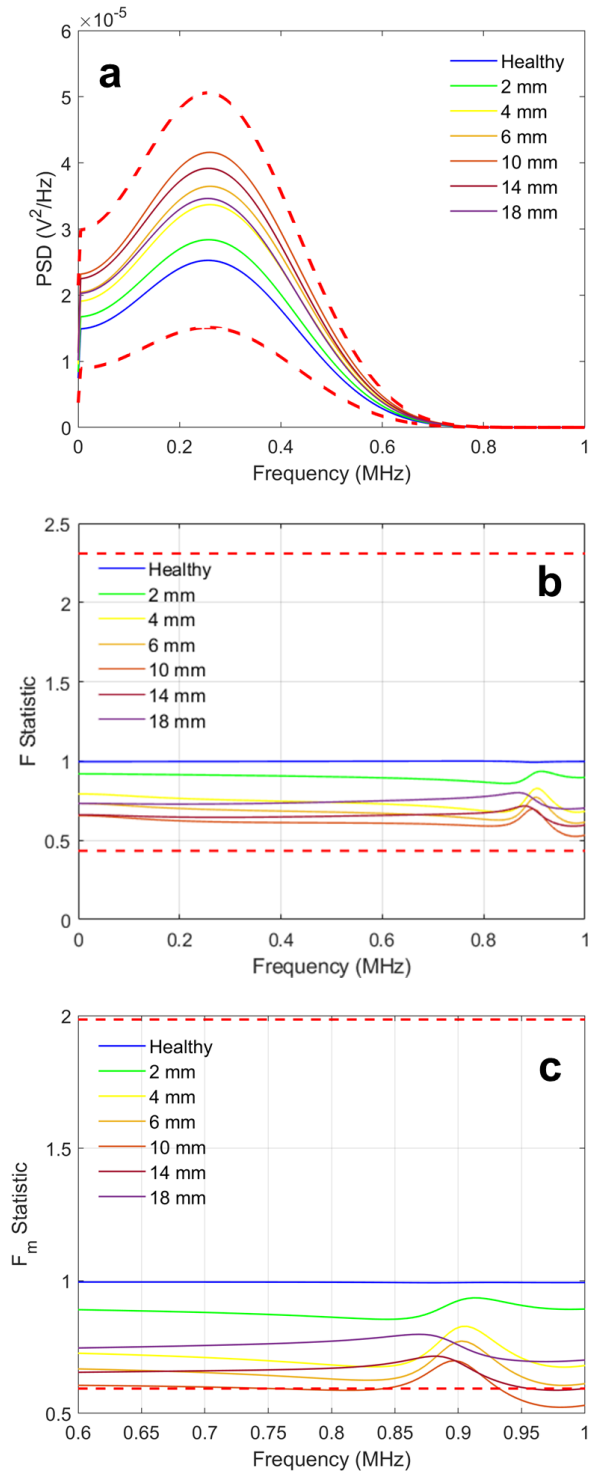

Fig. 8. Notched Al plate: Indicative damage detection results for S0 mode of path 5-1 (non-intersecting with damage) under 250 kHz actuation via the (a) F and (b) F_m statistics. The dashed horizontal lines indicate the damage thresholds at the 95% confidence level.

These observations can be explained in terms of the signals scattered off the damage from adjacent notch-intersecting paths. Indeed, as the damage-intersecting signal's energy is scattered, it is transferred to neighboring sensors, thus in-

Table 1. Missed fault percentages for notched Al plate under different damage cases and different actuator-sensor paths.

	2 mm		4 mm		6 mm		8 mm		10 mm		12 mm		14 mm		16 mm		18 mm	
Path	F	F_m	F	F_m	F	F_m	F	F_m	F	F_m	F	F_m	F	F_m	F	F_m	F	F_m
1-4	100	100	100	100	100	100	100	100	100	100	100	100	100	100	100	100	100	100
1-5	100	100	100	100	100	100	0	0	100	0	0	0	100	5	100	100	100	100
1-6	100	100	100	100	100	100	100	100	0	0	0	0	0	0	0	0	0	0
2-4	100	100	100	100	100	100	100	100	100	0	100	0	100	25	100	100	100	100
2-5	100	100	100	100	100	100	0	0	0	0	0	0	0	0	0	0	0	0
2-6	100	100	100	100	100	0	5	0	0	0	0	0	0	0	0	0	0	0
3-4	100	100	100	100	100	100	100	100	100	100	0	0	0	0	0	0	0	0
3-5	100	100	100	100	100	0	0	0	0	0	0	0	0	0	0	0	0	0
3-6	100	100	100	100	100	100	100	100	100	100	100	100	100	100	100	100	100	100

creasing the energy of the signals received at those sensors. In this context, as notch size increases, the amount of scattered energy increases, and thus the amount of energy added to the non-intersecting paths increases. However, also as the notch size increases, the angle of scattering changes, and at a large-enough notch length, the notch may become similar to a boundary, preventing scattered waves from reflecting to different parts of the plate. This might be the reason why the PSD drops after 10 mm. Nonetheless, the median PSD value for these extreme cases still stays larger than that for the healthy case. From this discussion, it becomes clear that the trends in the PSD with notch size can be used to indicate whether a given sensing path intersects damage or not.

Figure 9c shows the change in the STFT PSD magnitude with increasing notch size for the 2-6, 3-6, and 2-4 wave propagation paths. As shown, the general trend in sensing path 2-6 is the decrease in PSD with notch size compared to the healthy state, while an opposite trend can be observed with path 2-4 (even for notch sizes more than 10 mm) due to the aforementioned exchange of energy between signals. Also, path 3-6, being close to, yet not intersecting the notch, first exhibits a trend similar to the non-intersecting paths. After that, as the notch size increases and further intrudes the sensing path, a transformation in the PSD trend can be observed to more mimic that of a notch-intersecting path. Note that, although the same trend was observed for the paths relatively far from damage (paths 5-1 and 2-4), the distinct difference with path 3-6 is that the STFT PSD median actually decreases beyond the value of that of the healthy case for the 18 mm case.

From this indicative analysis, one can corner down the location of damage to within specific sensing paths, according to whether a given actuator-sensor path intersects or does not intersect damage. Furthermore, information from sensing paths that are close to damage (such as path 3-6 in this study) can be used to asses the damage evolution direction. All of this information can then be fed into damage localization algorithms reducing the amount of data that has to be analyzed, as well as producing more precise results. These are the topics of current research and will be presented via a comprehensive analysis in a future study.

Sub-scale Test: Stiffened Al Panel

In order to test the proposed non-parametric models in a more realistic situation, data collected over a stiffened Al panel, simulating part of a rotorcraft fuselage, was used to validate the methods presented herein. Figures 10a and 10b, respectively, present the full signal received at sensor 14 when sensor 5 was actuated (see Figure 2), as well as the second-arrival wave packet, for the different damage levels (DLs) in this study. Figure 10c shows the calculated DIs. As can be observed, although the DIs follow the evolution of the different DLs, giving a higher value with increasing damage level, the values of the DIs exhibit somewhat significant variations taking into account that the experiments took place in a laboratory environment. This pinpoints the need for a probabilistic active-sensing SHM framework that accounts for varying operating and environmental conditions. Furthermore, as shown in Figure 10c for DLs 3 and 4, damage quantification may not be straight forward using the DIs.

Figure 11a shows the Welch-based PSDs for path 5-14 using all 20 realizations per DL, where the dashed red lines show the theoretical 90% confidence intervals, while the dashed black lines show the experimental 90% confidence intervals. As can be seen, because 5-14 is a damage intersecting path, the PSD follows the evolution of the damage levels. The observed increase in signal PSD with DL can be explained in terms of the type of damage being inflicted on the component. Here, the different damage levels were designed to make the Al panel less stiffer at the point of damage, and thus it is expected that more energy can pass through that point as damage evolves. A second observation from Figure11a is that all DLs fall within the theoretical Welch-based confidence intervals (Ref. 29) of the healthy case, while almost all of them are deemed damaged when considering the experimental uncertainty. The latter observation is again expected due to the controlled lab environment, while the former observation has to do with the damages not having a large effect on the total energy reaching the sensors for the wave packet chosen in this study. The same trend can be observed with the F statistic (Figure 11b), which uses the theoretical estimation confidence intervals in the statistical decision-making process. That being said, the types of damage used in this study would have a much more pronounced effect had the stiffened panel been under load, which

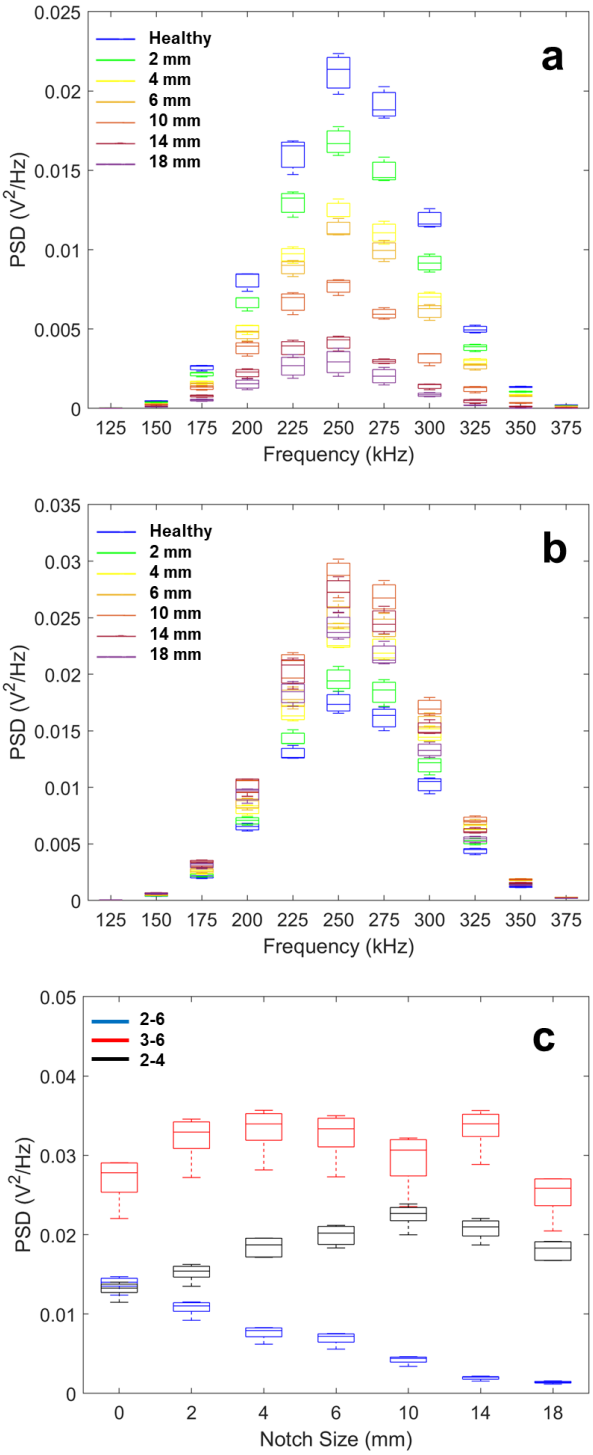

Fig. 9. Notched Al plate: The evolution of STFT-based spectral estimation under different notch sizes for actuator-sensor pair (a) 3-5 and (b) 5-1; (c) STFT estimation at 250 kHz for three paths under different damage cases. Boxplots indicate 95% confidence intervals.

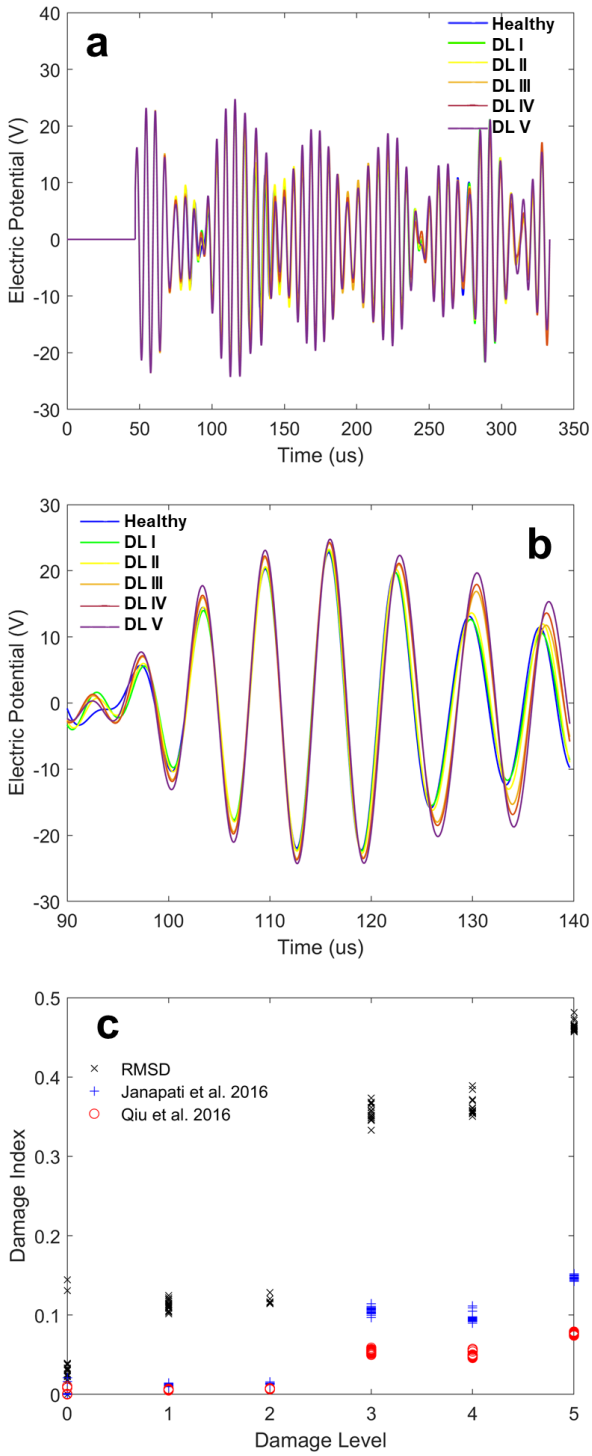

Fig. 10. Stiffened Al Panel: Indicative results from 5-14 signal path at 150 kHz actuation frequency for different damage levels (DLs); (a) the full signal, (b) the second arrival wave packet, and (c) the DI evolution using 20 realizations of the second-arrival wave packet for each DL.

is something that will be investigated in future work due to its relevance to the community.

Finally, Figure 11c indicates that the F_m statistic can detect the missing rivet, as well as all realizations of the last damage level (missing rivet and partially-popped rivet). This advantage that the F_m statistic has in detecting damage over the F statistic stems from the fact that the F_m statistic considers both: theoretical statistical confidence intervals, as well as ex-

perimental uncertainties, as incorporated in its formulation using the sample mean of the Welch-based PSD estimators obtained from multiple data sets. This combination has a synergistic effect in narrowing the theoretical confidence intervals using the "tighter" experimental ones. Note that, in the case of random vibration signals, the Welch-based PSD estimation yields theoretical confidence intervals that are much narrower than the corresponding experimental ones,which face challenges in capturing even minimal operational/environmental variability (Refs. 33, 35). In the case of active-sensing wave propagation, the nature of these signals is deterministic, thus the estimation of the Welch-based PSD statistics results in wider confidence intervals.

Following the same approach in the previous section, STFT spectral estimations were obtained for the Al stiffened panel using paths that both do and do not intersect damage, as respectively shown in Figures 12a and 12b. Again, the trend that can be observed for the damage-intersecting path is an increase in the PSD with damage level following the discussion above. As for the damage non-intersecting path (path 5-11 in Figure 12b), only a slight increase in PSD can be observed, which is attributed to the decreased attachment of the stringer to the panel in the event of damaged rivets, thus, again, allowing for more energy to pass through to the sensor on the other side. This increase, however, is significantly lower than that for the damage-intersecting path. This is clearly shown in Figure 12c where it can be observed that the rate of change of energy for the damage non-intersecting paths (in this case path 5-11 and path 5-15) is almost zero compared to that for path 5-14. These observations can again be used in cornering the location of damage.

CONCLUSIONS

In this study, a probabilistic framework for active-sensing guided-wave-based SHM was proposed using non-parametric time series models. Two damage detection methods based on corresponding statistical hypothesis tests were formulated using Welch-based PSD estimators: the first based on a single data set and the theoretical statistical properties of the Welch-based PSD, and the second based on a modified formulation that leverages the availability of multiple data sets per structural case for improved robustness under varying operating/environmental conditions. Furthermore, insights into probabilistic damage localization were extracted using the STFT spectral estimation. The proposed framework was applied to an Al notched plate with different notch sizes, as well as to a stiffened Al panel resembling a sub-scale rotorcraft fuselage component with different damage levels, including damaged and missing rivets. Using the developed statistical decision making schemes for the Al plate, notch sizes of at least 6 mm and 4 mm were correctly determined damaged using the first and second methods, respectively. Also, the advantage of the modified test that accounts for the availability of multiple data sets was apparent in the stiffened Al panel case, where the last two damage levels were detected using all available data sets, whereas the first method failed to detect

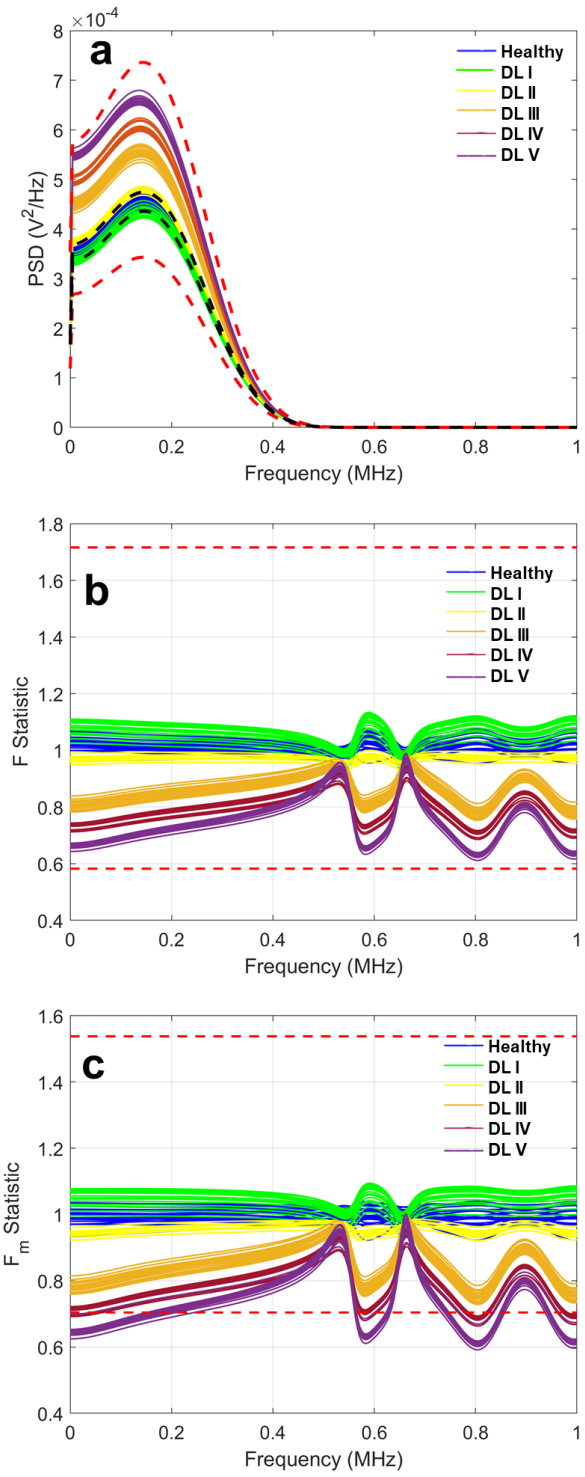

Fig. 11. Stiffened Al Panel: Indicative results for (a) the Welch PSD estimations for 20 realizations of the second-arrival wave packet of the path 5-14 for a 150 kHz actuation (the dashed red lines represent 90% estimation confidence intervals, while the black ones represent 90% experimental confidence intervals), and (b) F and (c) F_m statistics for the same data sets using 90% confidence levels.

damage. Using the proposed probabilistic framework, corresponding confidence intervals can be extracted for each case,

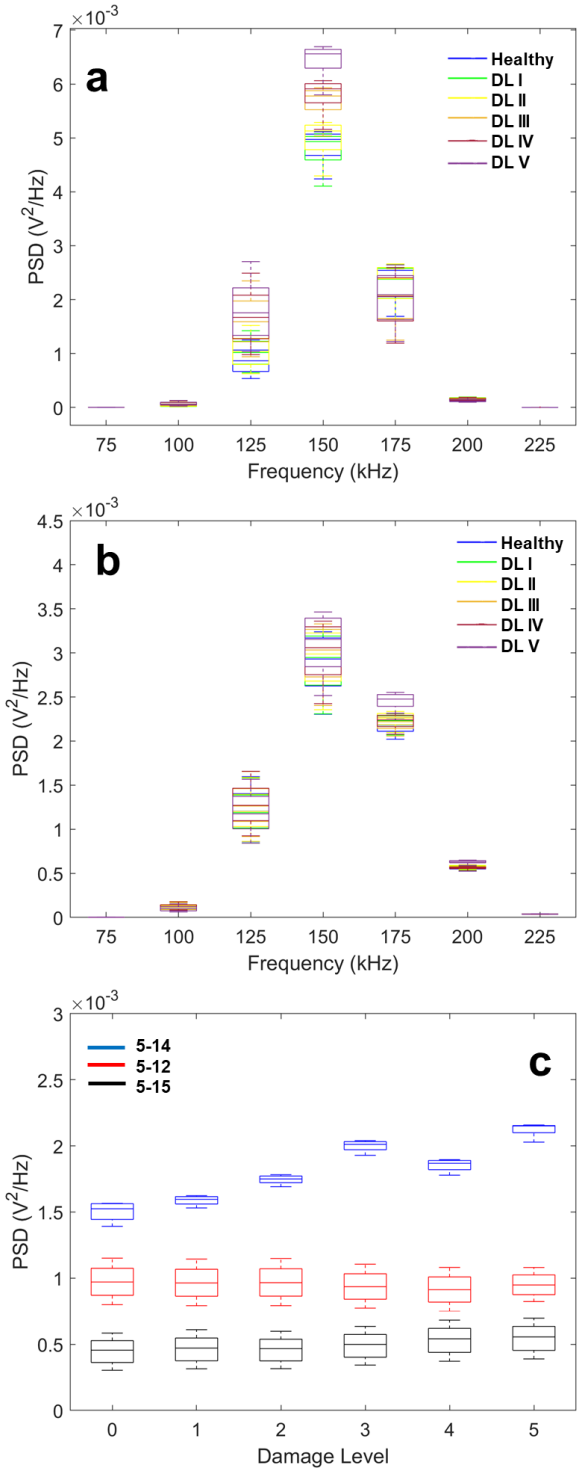

Fig. 12. STFT-based spectral estimation under different damage cases in the fuselage component for actuator-sensor pair (a) 5-14 and (b) 3-11. Panel (c) shows the evolution of the STFT with DL at 150 kHz for three actuator-sensor pairs.

adding a significant advantage in decision-making, as specific type I error probabilities can be explicitly defined, compared to the deterministic metrics being used today. In addition, for both components, a novel method using STFT estimation for cornering damage location to within specific actuator-sensor paths was presented based on the effect of damage on scattering wave energy. This method can be used for filtering unimportant information before feeding data into localization algorithms, making them more computationally-efficient and more accurate. In addition, this method can be used to identify potential "hotspot" locations on structural large-scale components.

Author contact: Ahmad Amer, amera2@rpi.edu; Fotis Kopsaftopoulos, kopsaf@rpi.edu

ACKNOWLEDGMENTS

This work is carried out at the Rensselaer Polytechnic Institute under the Army/Navy/NASA Vertical Lift Research Center of Excellence (VLRCOE) Program, grant number W911W61120012, with Dr. Mahendra Bhagwat and Dr. William Lewis as Technical Monitors.

REFERENCES

[1]Davis, M., Bouquillon, B., Smith, M., Allred, C., Sarjeant, R., Loverich, J., and Bordick, N., "Rotor load and health monitoring sensor technology," American Helicopter Society 71st Annual Forum Proceedings, Virginia Beach, Virginia, May 2015.

[2]LeFevre, B., Davis, M., Marr, C., Rusak, D., and Johnson, C., "Integrated Hybrid Structural Management System (IHSMS): usage and loads monitoring," American Helicopter Society 73st Annual Forum & Technology Display Proceedings, Fort Worth, Texas, May 2017.

[3]Schenck, E., Davis, M., Bond, R., Meyer, J., and Rusak, D., "Integrated Hybrid Structural Management System (IHSMS) aircraft impact monitoring," American Helicopter Society 73rd Annual Forum Proceedings, Fort Worth, Texas, May 2017.

[4]Kopsaftopoulos, F., Nardari, R., Li, Y.-H., and Chang, F.-K., "A stochastic global identification framework for aerospace structures operating under varying flight states," *Mechanical Systems and Signal Processing*, Vol. 98, 2018, pp. 425–447.
doi: 10.1016/j.ymssp.2017.05.001

[5]Spiridonakos, M. and Fassois, S., "Non-stationary random vibration modelling and analysis via functional series time-dependent ARMA (FS-TARMA) models–A critical survey," *Mechanical Systems and Signal Processing*, Vol. 47, (1-2), 2014, pp. 175–224.

[6]Zhang, Q. W., "Statistical damage identification for bridges using ambient vibration data," *Computers and Structures*, Vol. 85, 2007, pp. 476–485.

[7]Wilson, C. L., Lonkar, K., Roy, S., Kopsaftopoulos, F., and Chang, F.-K., "Structural Health Monitoring of Composites," *Comprehensive Composite Materials II*, edited by P. W. R. Beaumont and C. H. Zweben, Elsevier Ltd., 2018, pp. 382–407.

[8]Shah, A., Gunderson, K., Rimoli, J. J., and Ruzzene, M., "Closed loop approach to Structural Health Monitoring of critical rotorcraft components," American Helicopter Society 74th Annual Forum & Technology Display Proceedings, Phoenix, Arizona, May 2018.

[9]Ng, C.-T., "On the selection of advanced signal processing techniques for guided wave damage identification using a statistical approach," *Engineering Structures*, Vol. 67, 2014, pp. 50–60.

[10]Todd, M. D., Flynn, E. B., Wilcox, P. D., Drinkwater, B. W., Croxford, A. J., and Kessler, S., "Ultrasonic wave-based defect localization using probabilistic modeling," American Institute of Physics Conference Proceedings, Burlington, VT, May 2012.

[11]Flynn, E. B., Todd, M. D., Wilcox, P. D., Drinkwater, B. W., Croxford, A. J., and Kessler, S., "Maximum-likelihood estimation of damage location in guided-wave structural health monitoring," *Proceedings of The Royal Society A, Burlington, VT*, Vol. 467, (2133), 2011, pp. 2575–2596.

[12]Kay, S. M., *Fundamentals of Statistical Signal Processing: Detection Theory*, Prentice Hall: New Jersey, 1993.

[13]Haynes, C., Todd, M., Flynn, E., and Croxford, A., "Statistically-based damage detection in geometrically-complex structures using ultrasonic interrogation," *Structural Health Monitoring*, Vol. 12, (2), 2012, pp. 141–152.

[14]Yang, J., He, J., Guan, X., Wang, D., Chen, H., Zhang, W., and Liu, Y., "A probabilistic crack size quantification method using in-situ Lamb wave test and Bayesian updating," *Mechanical Systems and Signal Processing*, Vol. 78, 2016, pp. 118–133.

[15]He, J., Ran, Y., Liu, B., Yang, J., and Guan, X., "A Lamb wave based fatigue crack length estimation method using finite element simulations," The 9th International Symposium on NDT in Aerospace, Xiamen, China, November 2017.

[16]Peng, T., Saxena, A., Goebel, K., Xiang, Y., Sankararaman, S., and Liu, Y., "A novel Bayesian imaging method for probabilistic delamination detection of composite materials," *Smart Materials and Structures*, Vol. 22, 2013, pp. 125019–125028.

[17]Janapati, V., Kopsaftopoulos, F., Li, F., Lee, S., and Chang, F.-K., "Damage detection sensitivity characterization of acousto-ultrasound-based structural health monitoring techniques," *Structural Health Monitoring*, Vol. 15, (2), 2016, pp. 143–161.

[18]MIL-HDBK-1823A, "MIL-HDBK-1823A," *Nondestructive Evaluation System Reliability Assessment*, Department of Defense, April 2009.

[19]Gallina, A., Packo, P., and Ambrozinski, L., "Model Assisted Probability of Detection in Structural Health Monitoring," *Advanced Structural Damage Detection: From Theory to Engineering Applications*, edited by T. Stepinski, T. Uhl, and W. Staszewski, John Wiley and Sons, Ltd., 2013, pp. 382–407.

[20]Jarmer, G. and Kessler, S. S., "Application of Model Assisted Probability of Detection (MAPOD) to a Guided Wave SHM System," Structural Health Monitoring 2017: Real-Time Material State Awareness and Data-Driven Safety Assurance– Proceedings of the 12th International Workshop on Structural Health Monitoring (IWSHM 2017), edited by F.-K. Chang and F. Kopsaftopoulos, 2017.

[21]Kabban, C., Greenwell, B., DeSimio, M., and Derriso, M., "The probability of detection for structural health monitoring systems: Repeated measures data," *Structural Health Monitoring*, Vol. 14, (3), 2015, pp. 252–264.

[22]Moriot, J., Quagebeur, N., Duff, A. L., and Masson, P., "A model-based approach for statistical assessment of detection and localization performance of guided wavebased imaging techniques," *Structural Health Monitoring*, Vol. 17, (6), 2017, pp. 1460–1472.

[23]Kopsaftopoulos, F. P. and Fassois, S. D., "Vibration based health monitoring for a lightweight truss structure: experimental assessment of several statistical time series methods," *Mechanical Systems and Signal Processing*, Vol. 24, 2010, pp. 1977–1997.

[24]Kopsaftopoulos, F. P. and Fassois, S. D., "A Functional Model Based Statistical Time Series Method for Vibration Based Damage Detection, Localization, and Magnitude Estimation," *Mechanical Systems and Signal Processing*, Vol. 39, 2013, pp. 143–161.
doi: 10.1016/j.ymssp.2012.08.023

[25]Kopsaftopoulos, F. P. and Fassois, S. D., "Identification of Stochastic Systems Under Multiple Operating Conditions: The Vector-dependent Functionally Pooled (VFP) Parametrization," *under preparation for publication*, 2016.

[26]Ljung, L., *System Identification: Theory for the User*, Prentice–Hall, second edition, 1999.

[27]Petsounis, K. A. and Fassois, S. D., "Parametric Time-Domain Methods for the Identication of Vibrating Structures – A Critical Comparison and Assessment," *Mechanical Systems and Signal Processing*, Vol. 15, 2001, pp. 1031–1060.

[28]Box, G. E. P., Jenkins, G. M., and Reinsel, G. C., *Time Series Analysis: Forecasting & Control*, Prentice Hall: Englewood Cliffs, NJ, third edition, 1994.

[29]Kay, S. M., *Modern Spectral Estimation: Theory and Application*, Prentice Hall: New Jersey, 1988.

[30]Manolakis, D., Ingle, V. K., and Kogon, S. M., *Statistical and Adaptive Signal Processing: Spectral Estimation, Signal Modeling, Adaptive Filtering and Array Processing*, Artech House, New York, 2005, pp. 225–255.

[31]Manasas, M., Jane, R., Fiz, G. A., Morera, J., and Caminal, P., "Influence of estimators of spectral density on the analysis of electromyographic and vibromyographic signals," *Medical and Biological Engineering and Computing*, Vol. 40, 2002, pp. 90–98.

[32]Hayes, M. H., *Statistical Digital Signal Processing and Modelling*, John Wiley and Sons, New York, 1996.

[33]Kopsaftopoulos, F. and Fassois, S. D., "Vibration based health monitoring for a lightweight truss structure: experimental assessment of several statistical time series methods," *Mechanical Systems and Signal Processing*, Vol. 24, 2010, pp. 1977–1997.

[34]Kopsaftopoulos, F. P. and Fassois, S. D., "Experimental assessment of time series methods for structural health monitoring (SHM)," Proceedings of the 4th European Workshop on Structural Health Monitoring (EWSHM), 2008.

[35]Kopsaftopoulos, F. P. and Fassois, S. D., "Vibration Based Health Monitoring for a Thin Aluminum Plate – A Comparative Assessment of Statistical Time Series Methods," Proceedings of the 5th European Workshop on Structural Health Monitoring (EWSHM), 2010.

[36]Qiu, L., Yuan, S., Bao, Q., Mei, H., and Ren, Y., "Crack propagation monitoring in a full-scale aircraft fatigue test based on guided wave Gaussian mixture model," *Smart Materials and Structures*, Vol. 25, 2016, pp. 055048.